Ionization loss for high-energy electrons in thin targets*

James T. O'Brien,† Hall Crannell, and F. J. Kline‡
Department of Physics, The Catholic University of America, Washington, D.C. 20017

S. Penner
National Bureau of Standards, Washington, D.C. 20234

(Received 15 October 1973)

The most-probable ionization loss has been measured for relativistic electrons passing through thin absorbers of carbon, aluminum, and copper. Incident energies of 50 and 100 MeV were used. Target thicknesses ranged from 48 to 614 mg/cm^2 and encompass the range of thicknesses most frequently used in electron scattering experiments at these energies. The measured values of the most-probable ionization losses are in good agreement with the theoretical predictions of Sternheimer. The techniques for using values of the ionization loss to determine the target thickness in electron scattering experiments are presented.

[NUCLEAR REACTIONS Nat. C, Al, Cu (e,e'), $E=50$, 100 MeV; measured most-probable energy loss for electrons.]

I. INTRODUCTION

The energy lost by a relativistic electron while traversing a layer of matter may be given off as electromagnetic radiation, or it may be transferred to the nuclei or to the atomic electrons of the material. The total of energy transferred to the atomic electrons is often called the "ionization loss," and this nomenclature will be used throughout this paper. It must be noted that interactions in which an atomic electron is excited to a higher-energy *bound* state are included in this quantity, along with those interactions which actually lead to the production of an ion pair.

A number of experimental studies of ionization losses for high-energy (>10 MeV) electrons have been reported since the early 1950's. The results of some of these studies are discussed briefly in Sec. II of this paper. The theory of ionization loss has been extensively developed by Sternheimer.[1] Comprehensive review articles on work in this field, both experimental and theoretical, have been compiled by Price[2] and, more recently, by Crispin and Fowler.[3]

None of these earlier experiments involved measurements on targets as thin as those typically employed in high-resolution electron scattering studies. The present experiment was performed to check the ionization loss predictions for these thinner targets and to investigate the possibility of using these measurements to determine the target thickness simultaneously with the electron scattering data. This work thus extends measurements of ionization loss for 50- and 100-MeV electrons to thinner targets of carbon, aluminum, and copper than have been used in previous measurements with a greater precision than any previous work.

Section III of this paper presents the theoretical equations for ionization loss in a form which was convenient for this experiment. The experimental techniques are described in Sec. IV and, finally, the data and conclusions appear in Sec. V.

II. BACKGROUND

Experimental investigations of energy losses through ionization have covered a wide variety of incident particles, energies, target materials, and target thicknesses. Except for the earliest work related to the development of the theory, the discussion here will be restricted to high-energy electrons in relatively thin targets.

In the early 1950's several measurements were performed using low-energy (0.6- to 15.7-MeV) electrons. Goldwasser, Mills, and Hanson,[4] Hildebrand,[5] and Paul and Reich[6] all reported measurements which gave a better fit to the theory if target-density effects were included. Goldwasser, Mills, and Robillard[7] observed the density effect directly by performing experiments on the same polycarbonates in both solid and gaseous forms.

One of the earliest experiments to use 100-MeV electrons was the work of Hudson.[8] Titanium, beryllium, carbon, and aluminum targets of thickness ~2.0 g/cm^2 were investigated. The most-probable ionization loss and the full width at half maximum (FWHM) of the distribution were both found to be in reasonable agreement with theory.

More recent experiments include the work of Bumiller, Buskirk, Dyer, Miller, and others,[9]

on Al, Cu, and Pb targets of thickness from 0.7 to ~6.0 g/cm^2 using incident energies from 50 to 100 MeV. Radiative losses as well as ionization losses were included in measuring and computing the most-probable total-energy loss and the FWHM. Good agreement with theory was reported except for the values of the FWHM obtained from the thickest targets.

Theissen and Gudden[10] have reported measurements using 53-MeV electrons on carbon targets of thickness 0.3 to 5.0 g/cm^2. Their experiment, which comes closest to the thickness range under consideration in the present work, also obtained agreement with theoretical values of most-probable ionization loss within an uncertainty of ~5%.

III. THEORY

The theory of ionization loss is concerned with the prediction of various parameters which describe the energy distribution to be expected when an initially monoenergetic beam of particles passes through a sample of matter of known thickness. As an example, the most common parameters for describing a symmetric distribution would be its mean value and its width. The ionization-loss distribution, however, is not symmetric due to the fact that there is a finite probability for any given particle to lose any amount of energy from zero up to its total incident energy. This distribution, shown schematically in Fig. 1, was first described in detail by Landau[11] and is called "Landau straggling." The parameters most frequently used to describe the Landau distribution are the average energy loss ($\bar{\epsilon}$), the most probable energy loss (ϵ_p), and the full width at half maximum.

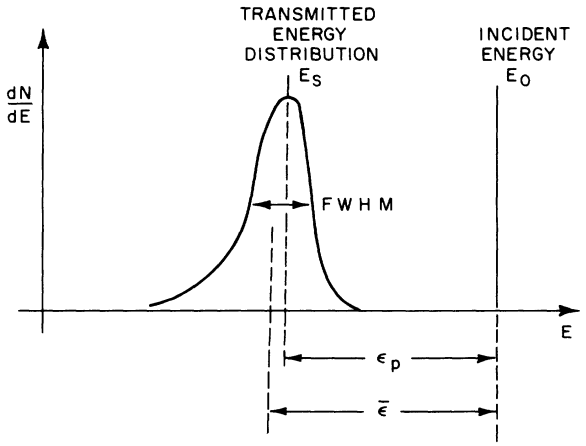

FIG. 1. A sketch of the Landau straggling distribution, showing the average energy loss ($\bar{\epsilon}$) and the most-probable energy loss (ϵ_p).

Maccabee and Papworth[12] have done more accurate numerical computations of the most-probable energy loss and have shown that a term 0.373 in the original Landau formula should be replaced by the value 0.198. This results in a new value of 0.891 for the constant previously evaluated as 1.06 in the expression for ϵ_p as given by Sternheimer.[1] Sternheimer and Peierls use this new value in a recent paper[13] in which the expression for ϵ_p for electrons appears as

$$\epsilon_p = \frac{At}{\beta^2}\left(B + 0.891 + 2\ln\frac{p}{m_e c} + \ln\frac{At}{\beta^2} - \beta^2 - \delta\right), \quad (1)$$

where

$$A = \frac{2\pi N e^4}{m_e c^2}\frac{Z}{A_0} = 0.1536\frac{Z}{A_0}\ \text{MeV cm}^2/\text{g}. \quad (2)$$

N is Avogadro's number, e is the charge on an electron, m_e is the mass of an electron in MeV/c^2, c is the velocity of light, Z and A_0 are the average atomic number and mass of the target material, respectively. $\beta = v/c$ where v is the velocity of the electron.

$$B = \ln\left[m_e c^2(10^6)/I^2\right], \quad (3)$$

where I is the average ionization potential (in eV) of the target atoms. p is the momentum of the incident electrons, t is the target thickness in g/cm^2, and δ is the density correction which is given by

$$\delta = 2\ln\frac{p}{m_e c} + C + a(X_1 - X)^m, \quad X_0 < X < X_1,$$
$$\delta = 2\ln\frac{p}{m_e c} + C, \quad X_1 < X, \quad (4)$$

where $X = \log_{10}(p/m_e c)$, and C, a, m, X_0, and X_1, are constants which depend on the material being studied and have been tabulated by Sternheimer for many substances.[1]

The constant C in the density effect can be written

$$C = -2\ln\left(\frac{I}{h\nu_p} - 1\right), \quad (5)$$

where

$$\nu_p = \left(\frac{e^2}{\pi m_e}\frac{N\rho Z}{A_0}\right)^{1/2}, \quad (6)$$

and ρ is the target density in g/cm^3. Now in the relativistic limit, where $\beta \simeq 1$, it is possible to use Eqs. (2) through (6) to rewrite Eq. (1) in the particularly simple form

$$\epsilon_p = At\left[K + \ln\frac{t}{\rho} - a(X_1 - X)^m\right], \quad X_0 < X < X_1 \quad (7a)$$

or

$$\epsilon_p = At\left(K + \ln\frac{t}{\rho}\right), \quad X_1 < X, \tag{7b}$$

where K is a constant equal to 19.26.

Equation (7b) is valid for all of the carbon data reported in this paper. The aluminum and copper targets require the use of Eq. (7a). The values of $K - a(X_1 - X)^m$ for the aluminum and copper targets differ only slightly from 19.26, as is shown in Table I.

IV. EXPERIMENTAL PROCEDURES

A. Target thickness

The parameter of interest in describing a target was its thickness in the region through which the electron beam was passed. This thickness was obtained by two sets of measurements. The average thickness was measured in units of mg/cm^2 in a simple and straightforward fashion. The target was weighed on an analytical balance and its cross-section area was carefully measured with vernier calipers. Uncertainty in these measurements was generally <0.2%. An x-ray photograph of the target was then used to compare the thickness in the vicinity of the electron beam with this over-all average.

In producing films of the targets it was desired to choose the mean incident energy such that maximum contrast in exposure density would be obtained. The intensity of electromagnetic radiation g, which is transmitted through a thickness of material t, is given by the expression

$$g = g_0 e^{-\mu_0 t},$$

where g_0 is the incident intensity and μ_0 is the mass absorption coefficient. Maximum contrast implies that dg/dt is to be maximized. For a given thickness and Z, the maximization is performed by varying μ_0, which is a function of the incident energy. The desired incident energy is that for which $\mu_0 = 1/t$. Plots of the attenuation coefficient vs incident energy, found in Evans,[14] were used to assist in estimating the optimum x-ray energy for each target.

The actual procedure in obtaining the x-ray pictures involved first taking a group of exposures at the estimated energy, adjusting current and exposure time to obtain satisfactory over-all film density. These time and current values were then maintained while the energy was readjusted to maximize contrast. Since the optimum value of μ_0 varies strongly as a function of Z (approximately $Z^{4.5}$) but varies only as the inverse of the thickness, future exposure on targets of any element required only an adjustment of the exposure time in proportion to the thickness of the target. The range of thickness investigated in the experiment was not so large as to appreciably affect the optimum energy setting.

TABLE I. Density-correction contribution.

Material	Energy (MeV)	$K - a(X_1 - X)^m$
Aluminum	50	19.17
Aluminum	100	19.23
Copper	50	19.16

Small pieces of very thin foils of the same Z (or very nearly the same) as the target being studied were used to provide calibration steps on the films. Thus, optical-density variations from point to point on the film could be directly related to the thickness of the calibration foil. These foil steps were placed on top of the target so that the observed change in the optical density did, in fact, represent the effect of a small thickness change superimposed on the target in this region.

Analysis of the x-ray films of the actual targets used in the experiment was performed with the aid of a scanning microdesitometer. Scans covering the entire width of each target were made at a number of equally spaced positions across its height. Care was taken to see that at least one of these scans passed across the region through which the electron beam would travel. In most cases, additional scans were taken in this central region in order to observe any short-range fluctuations which would be averaged over by the size of the electron-beam spot.

Each of these scans was subdivided into intervals corresponding to a distance of 4 mm on the target. The average value of relative optical density within each of these intervals was then recorded. Each of these numbers corresponded to the mean density on the film within a rectangular box of dimensions 4 mm (determined by scanning motion) $\times$0.5 mm (provided by vertical aperture setting), which are the approximate dimensions of the electron-beam spot at the target plane. These small rectangles were in turn distributed on a rectangular grid across the entire target. The average of these measurements was taken to be the average optical density of the target.

Once the average film density had been determined it was a simple matter to compare this with the film density at the center of the target and, by use of the calibration steps previously described, to determine the actual thickness in the region through which the beam would be passed. Of all the targets investigated, only four were found to have central regions which differed from the aver-

age thickness by more than 0.1%, the largest difference being 0.41% on one of the carbon targets.

B. Analysis of scattering data: General techniques

1. *Introduction*

The energy-loss measurement was performed at the electron scattering facility of the National Bureau of Standards' Center for Radiation Research. In this system, scattered electrons are counted by an array of semiconductor detectors located at the focal plane of a double-focusing magnetic spectrometer. The detector array, called the ladder, can be moved along the focal plane. The momentum of a scattered electron is thus determined from the detector in which it was counted, the detector ladder position, and the setting of the spectrometer field. This facility is described in detail in a series of National Bureau of Standards (NBS) documents.[15]

In performing the energy-loss measurement at NBS it was not practical to observe the electrons which passed straight through the target without scattering. Major modifications to the vacuum system, and the removal of the Faraday-cup current monitor, would have been required in order to move the spectrometer to the 0° position. It would then have been necessary to hold the beam steady on target at a current low enough to avoid jamming of the detectors. The experiment was therefore performed using a scattered (and hence reduced intensity) beam.

In the course of these measurements several different target-beam geometries were employed. There were, however, a great many data analysis procedures common to all geometries, e.g. the production of normalized spectra of scattered electron energies and the location of peak centers in these spectra. These techniques will be described first, followed by more detailed discussions of the individual geometries and of the considerations which led to changes from one geometry to another.

2. *Production of spectra*

The data were first analyzed by a general data-reduction program which is described in more detail elsewhere.[16] This program is designed to produce complete energy spectra for every target from which scattering is performed at a particular incident energy and scattering angle. The raw data or counts are normalized, and corrected for counting rate and for relative efficiencies of the various detectors.

A "raw" spectrum produced by this basic program contains a data point for each detector for every position of the detector ladder at every spectrometer current setting. A three-parameter bin-sorting routine was used to reproduce the shape of this raw spectrum with a set of points which were evenly spaced along the energy axis. The spectrum was then corrected for energy loss via radiation. Schwinger[17] and thick-target bremsstrahlung contributions were both included. These radiative corrections were performed by a spectrum stripping technique which has been described in Ref. 18.

3. *Peak fitting*

Common to all target geometries was the problem of accurately locating the centers of peaks in the energy spectra. Since the bin-sorted spectra could, in most cases, be produced reliably at a bin width of 10 keV it was always possible to locate the maximum value of a peak to within ±5 keV simply by observation. It was desired, however, to work at considerably greater precision than this and a way was sought to locate these maxima to ±1 keV. A computer program was written which would fit a parabola, by a least-squares calculation, to three or more data points centered about the peak. The coordinate of the axis of symmetry of the parabola, and its uncertainty due to the statistical uncertainties associated with the data points being fitted, were then found. A χ^2 subroutine was included in order to indicate how well each set of data points was fitted by the parabolic shape.

The program was applied to the analysis of peaks in the radiative unfolded spectra. This was considered to be a safe procedure because the statistical uncertainties on the raw data had been propagated through both the bin-sorting and the unfolding computations. To insure against the possibility that information was being either added or lost by the application of two successive interpolations (once in the bin sort and again in peak fitting) a number of checks were made. The checking procedure involved applying the peak-fit program directly to the raw spectrum for a particular data set and then to the bin-sorted (but not unfolded) spectrum for the same data set. The centers of these two peaks were always found to be in agreement with each other to better than $\pm\frac{1}{2}\%$ of the value of ϵ_p for the data set in question.

4. *Beam-width correction*

The theoretical expression derived in Sec. III [Eqs. (7)] is used to predict the most probable energy loss which will result if a *monoenergetic* beam of relativistic electrons is passed through a target of known thickness. The beam from the accelerator, however, has a finite range of energies within it, i.e., it has an energy distribution. Thus,

the peak shape observed in the bin-sorted and radiative corrected spectrum was, in fact, a convolution of the distribution produced by ionization losses with the distribution of the incident beam. Since at least one of these distributions is known to be asymmetric, i.e., the Landau distribution, it follows that the resultant distribution is not only wider than the theoretical case but shifted in position as well.

Figure 2(a) shows the theoretical situation. A monoenergetic beam of electrons, indicated by a vertical line at E_0, when incident upon a target of known thickness will produce the transmitted energy distribution given by Landau. The energy difference between the incident beam and the maximum point of the transmitted distribution is the most-probable energy loss ϵ_p which we seek to measure experimentally.

Figure 2(b) shows an experimental situation in which the monoenergetic beam is replaced by a beam with a symmetric distribution of energies, centered on the value of the theoretical incident energy. The observed transmitted distribution is wider than the theoretical case and its maximum point is displaced by a greater amount. Thus the distance between the centers of the two peaks in Fig. 2(b), which is the quantity that can be measured by the experimental procedures so far described, is larger than the theoretically predicted value of ϵ_p by an amount which depends on the width and the shape of the energy distribution of the incident beam.

To correct for the beam-folding effect a computer simulation of the folding process was devised. This program accepted two functions and computed their convolution by a "boxcar integration" technique. The peak-fitting program was then used to locate the centers of each of the three functions. The difference in position of the Landau peak and of the convolution peak with respect to the center of the beam distribution could then be used as a measure of the energy shift which would be introduced by this particular beam shape.

In the process of investigating these beam-folding effects, a variety of different shapes were used to represent the beam distribution. These shapes are shown in Fig. 3 and will be referred to in more detail below. In Fig. 4 the energy shift due to beam-folding effects is plotted in units of percentage of the width of the incident beam. The abscissa is the ratio of the widths of the Landau distribution and the beam distribution. The largest shifts are observed to occur in the region where the two functions being folded have essentially equal widths. This is to be expected because, as the width ratio approaches either extreme, the narrower shape begins to look more and more like a δ function as compared with the wider.

A detail common to all target geometries was the use of the scattered electrons from a very thin beryllium foil as a means of determining the incident energy. It was hoped that the shape of this elastic peak could be related to the incident beam profile. The shapes used in generating Fig. 4 therefore include an uncorrected Be elastic peak, a radiative unfolded Be peak, and an artificial peak (labeled fake beam) produced by taking the data on the high-energy side of a Be peak and reflecting these same data to obtain the low-energy side in order to force a symmetric shape.

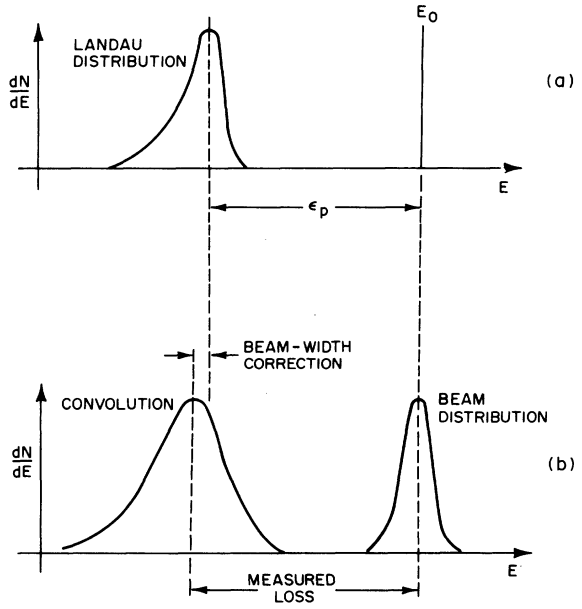

FIG. 2. The dependence of the most-probable energy loss on the incident energy distribution.

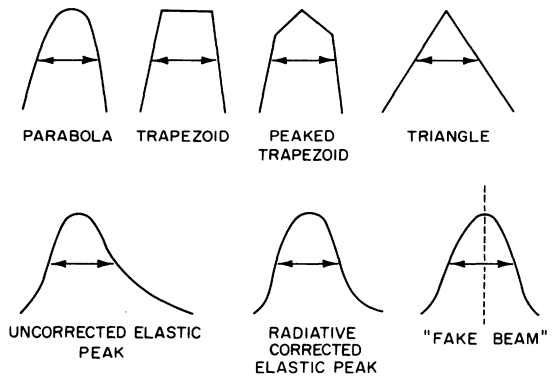

FIG. 3. Some sample profiles used as beam distributions in the investigation of the beam-width dependence.

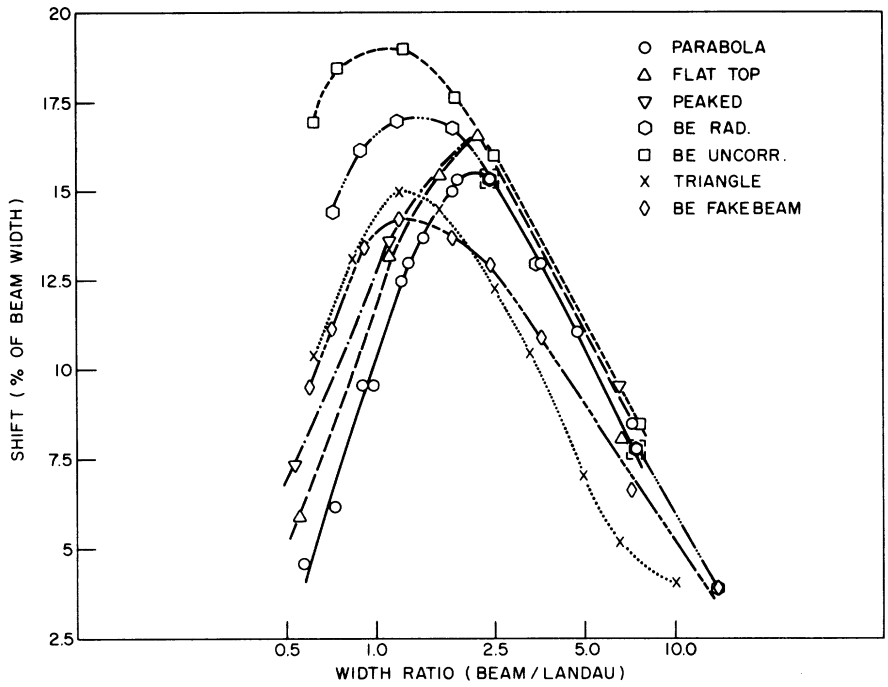

FIG 4. The dependence of the beam-width correction on the shape of the incident distribution. The various curves correspond to the test distributions shown in Fig. 3.

C. Target-beam geometries

At the time that the ionization-loss project was initiated it was hoped that a method might be developed whereby the experimental measurement of the most-probable energy loss in a scattering target could be used as a measure of the effective thickness of that target. For this reason the initial work was performed using target arrangements in which the absorber material was located in the beam, at the location where the target would normally be placed for a scattering experiment. Final data on the thinner targets were taken with the absorber material out of the direct beam from the accelerator, since this latter method involved fewer sources of experimental uncertainty.

1. Geometry No. 1

The first arrangement of targets in the electron beam is shown in Fig. 5. In this geometry the beam could be made to strike either of two positions within the target frame by moving the entire target ladder vertically across the path of the beam. Figure 5(b) shows schematically an elevation view of the edge of the target. In the position labeled α the beam passes through only the thin beryllium reference foil. In the β position the beam strikes both the reference foil and the thicker absorber.

An elevation view of the face of the target itself is shown in Fig. 5(c). The entire opening within this frame is covered with a thin Be foil, generally 0.0046 g/cm^2 thick. This foil, which is used to determine the energy of the incident beam, will be

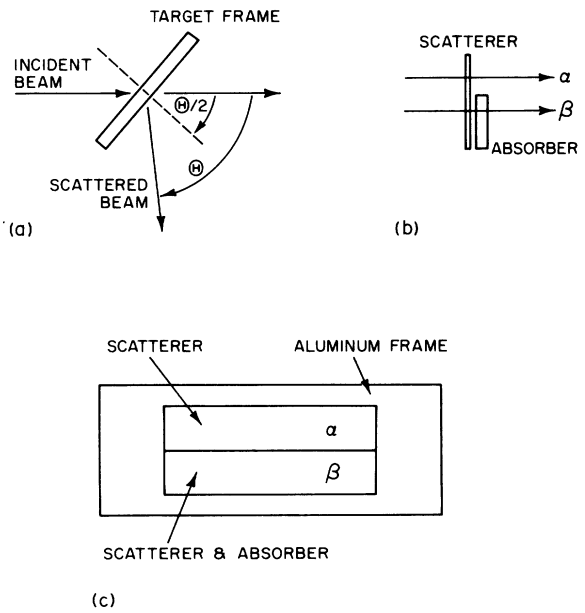

FIG. 5. Views of the target arrangement for geometry No. 1.

frequently referred to hereafter as the "scatterer." On top of this foil is laid the thicker foil on which the energy-loss measurement is to be made. This thicker foil, which shall be called the "absorber," is just large enough to cover the lower half of the opening.

A plan view of the path by which the beam intercepts these targets is shown in Fig. 5(a). The target frames are placed in the vacuum chamber at an angle such that the normal to the plane of the target bisects the angle through which the observed electrons are scattered. This is called the standard transmission geometry for electron scattering. Every electron scattered toward the spectrometer passes through the same thickness of target material, independent of how deeply it had penetrated into the target prior to scattering.

The type of scattered-energy spectra obtained for beam positions α and β is shown in Fig. 6. The α spectrum contains only the peak for electrons elastically scattered from beryllium. The β spectrum, on the other hand, contains two peaks corresponding to elastic scattering from the absorber nuclei as well as from the Be. The separation between the peaks in the β spectrum is due to the difference between the energy lost to recoil of the Be nuclei and to recoil of the heavier absorber nuclei. The absorber peak is much larger than the scatterer peak due to the much larger number of absorber nuclei which are present and to the Z^2 dependence of the elastic scattering cross section.

The relative positions of the absorber peak in the β spectrum and the scatterer peak in the α spectrum will depend on the mass of the absorber nuclei and the thickness of the absorber. The scatterer peaks in the two spectra, however, were produced by scattering from the same piece of beryllium, and hence their energy separation is due entirely to the presence in case β of the additional thickness of the absorber material. Thus it is only necessary to apply the beam-folding corrections to the measured separation between these peaks in order to obtain the value of ϵ_p for the absorber in question.

The attractive feature of this method, then, is the fact that comparison of the two spectra yields a direct measurement of ϵ_p without any need to account for recoil losses or Schwinger radiation. Practical limitations on this method are the low counting rates in the scatterer peak in spectrum β, and the large absorber radiative tail which must be carefully subtracted from beneath the scatterer peak in this same spectrum.

2. *Geometry No. 2*

It is possible, by taking recoil into consideration, to arrive at a measure of most-probable energy loss by an investigation of the elastic peak position of the absorber compared with that of the scatterer. The data in this case are taken by substituting the two targets in the beam at the standard transmission angle, maintaining the same settings of all parameters which control the energy of the incident beam.

The method for analysis of data taken by this substitution procedure can be divided into five steps. These steps are diagrammed in Fig. 7. In the description that follows, the individual steps are enumerated in correspondence with this dia-

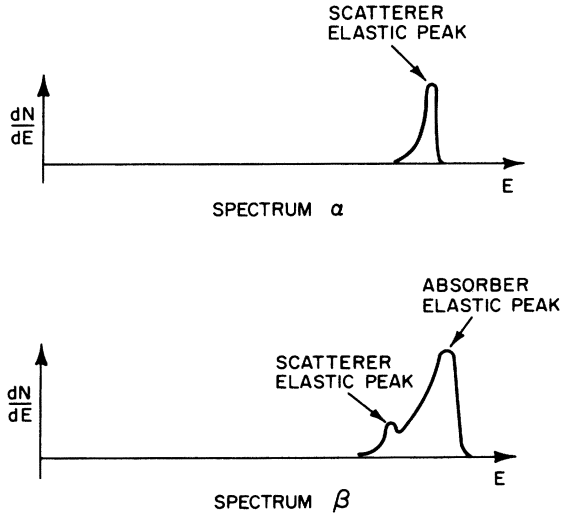

FIG. 6. The types of spectra obtained in geometry No. 1.

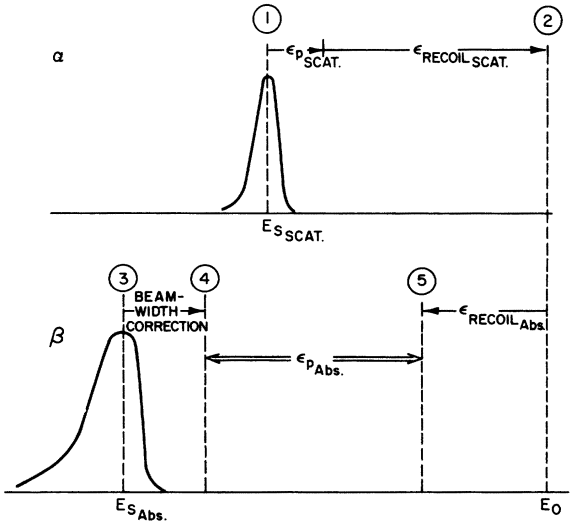

FIG. 7. A diagram of the data-reduction procedure for geometry No. 2.

gram:
(1) A bin-sorted and radiative-unfolded spectrum from the Be scatterer is produced. The center of the elastic peak ($E_{s_{scat}}$) is located by the parabolic fitting program.
(2) Corrections are made for energy losses to recoil and to ionization in the beryllium target, in order to obtain the value of the incident energy (E_0). Since the ionization losses in these Be targets are quite small (~5 keV), any uncertainty in these numbers represents a very small perturbation in the value of E_0. These corrections are combined by assuming that the scattering takes place at the midpoint of the target thickness, according to the following expression:

$$E_0 = \frac{E_s + \frac{1}{2}\epsilon_p}{1 - [2(E_s + \frac{1}{2}\epsilon_p)/M_t c^2] \sin^2 \frac{1}{2}\theta} + \frac{1}{2}\epsilon_p, \qquad (8)$$

where $M_t c^2$ is the target mass in MeV, and E_s represents $E_{s_{scat}}$.
(3) A bin-sorted and radiative-unfolded spectrum from the absorber is produced and the center of the elastic peak ($E_{s_{abs}}$) is located.
(4) The beam-folding correction is applied to $E_{s_{abs}}$.
(5) The value of ϵ_p in the absorber is obtained by solving Eq. (8) for ϵ_p, and evaluating the resulting expression using the measured value of E_0 (from step 2) and the beam width corrected value of $E_{s_{abs}}$ (from step 4).
This method is particularly useful with respect to the secondary goal of using the ionization-loss measurement to determine target thickness, since the only data required beyond the actual electron scattering spectrum from the target of interest is the elastic scattering peak from a separate beryllium target.

A significant disadvantage to the substitution method lies in the uncertainty involved in selecting the appropriate beam profile to be used in making the beam-folding correction. Since the width of the Landau distribution produced by the Be scattering is quite small it was considered to be a reasonably safe assumption that the observed Be peak, once corrected for radiative losses, should give a good representation of the beam profile. The uncertainties introduced by this procedure were found to be of the order of ±1 keV, more or less independent of absorber thickness. This was considered acceptable for the thicker targets having $\epsilon_p \geq 200$ keV, as it represented less than 1% effect. In the interests of obtaining the maximum available precision, however, it was decided to use a new target arrangement which would remove even this uncertainty.

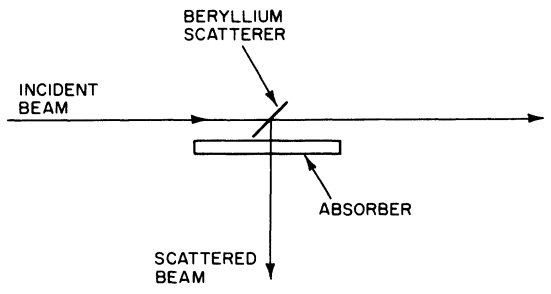

FIG. 8. A plan view of the target arrangement for geometry No. 3.

3. *Geometry No. 3*

This arrangement, like geometry No. 1, utilized a comparison of elastically scattered electrons from a thin Be target along two alternate paths. In one case, spectrum α, the scattered electrons passed directly into the spectrometer while in the second case, spectrum β, the electrons passed through the absorber material on the way to the spectrometer. The problems of geometry No. 1 were eliminated by the simple expedient of removing the absorber material from the path of the incident beam. A plan view of this arrangement is shown in Fig. 8. This geometry is very similar to target arrangements reported in earlier ionization-loss measurements.[9,10]

The beam-folding correction can now be performed with confidence because the energy distribution incident on the absorber is known to be precisely that distribution which is scattered from the beryllium and which appears in spectrum α. The radiation correction in this case must be performed only for the very small contribution from thick-target bremsstrahlung as the electrons traverse the absorber, since this is the *only* radiation loss which takes place *after* the electrons leave the scatterer. Thus, it is only necessary to locate the centers of the peaks in spectra α and β, apply the beam-folding correction to β, and record the remaining energy difference as ϵ_p for the absorber in question.

The primary advantages of this arrangement, then, are the precise knowledge of the beam-folding correction and the minimization of radiation contributions to the peak position.

V. RESULTS AND DISCUSSION

A. Introduction

The results of the measurements of most-probable energy loss are compared with theoretical values of Table II. The uncertainties in theoretical values indicated in this table are due to the uncertainty in target thickness. The uncertainties tabulated for the experimental values are 1 standard deviation estimates on the energy-loss mea-

TABLE II. Most-probable ionization losses for all data.

No.	Element/ geometry	Incident energy (MeV)	Effective thickness (mg/cm^2)	ϵ_p Theoretical (keV)	ϵ_p Experimental (keV)	Difference (%)
1	C/3	50	47.7± 0.9	57.7± 1.0	61.9±1.6	7.3 ±4.8
2	C/3	50	72.4± 1.4	89.9± 1.8	92.9±1.6	3.3 ±3.5
3	C/3	50	85.9± 1.6	107.8± 2.0	113.1±1.6	4.9 ±3.0
4	C/3	100	85.9± 1.6	107.8± 2.0	114.5±1.8	6.2 ±3.1
5	C/3	50	95.5± 1.8	120.6± 2.4	121.3±1.6	0.6 ±2.9
6	C/2	50	204 ± 2	269.5± 2.5	273.8±2.5	1.6 ±1.5
7	C/2	50	454 ± 5	627.6± 7.0	635.0±2.7	1.2 ±1.2
8	C/2	50	614 ±12	863.0±17.	855. ±4.7	−0.9 ±2.0
9	Al/3	50	61.1± 1.2	69.5± 0.9	67.9±2.9	−2.3 ±5.2
10	Al/2	50	88.5± 1.7	103.2± 2.2	100.9±1.7	−2.2 ±3.3
11	Al/1	100	88.9± 1.7	104.1± 2.2	105.9±2.5	1.71±3.7
12	Al/3	50	122.0± 2.4	145.1± 3.0	149.5±2.4	3.0 ±2.9
13	Al/1	100	179.3± 3.5	219.2± 4.6	222.1±1.5	1.3 ±2.4
14	Al/3	50	247.5± 4.8	307.3± 6.4	319.6±1.9	4.0 ±2.2
15	Al/2	50	269.2± 5.2	335.9± 7.0	333.7±1.7	−0.6 ±2.1
16	Al/1	100	358.0± 6.9	454.3± 9.5	453.3±4.3	−0.2 ±2.3
17	Cu/3	50	60.9± 1.2	60.5± 1.2	62.5±1.6	3.3 ±4.7
18	Cu/3	50	120.9± 2.4	225.9± 2.4	129.7±1.7	3.0 ±2.8

surement and do not include systematic effects (see below). The combined uncertainty in the % difference column does include the systematic contribution. The data entries are consecutively numbered for easy reference.

B. Major corrections

1. Beam width

The beam-width correction has been described in some detail in the previous section. In making this correction for geometries 1 and 2, the radiative-unfolded beryllium elastic peak from the scatterer spectrum was used as the best available estimate of the incident energy distribution. For geometry 3 the incident distribution was measured directly (spectrum α) and hence was accurately known.

The size of this correction is tabulated for all 18 data sets in Table III. It will be noticed that entries 4, 11, 13, and 16 (the 100-MeV data sets) exhibit the largest shifts. The remaining values can be seen to display the behavior described in Sec. IV, reaching a maximum value near the center of the thickness range as the Landau width begins to exceed the beam width. The experimental shifts are plotted *vs* the ratio of beam/Landau widths in Fig. 9 for comparison with Fig. 4.

2. Beryllium thickness

In the experimental arrangement for geometries 1 and 3, one piece of thin Be foil is used to provide the reference peak (the α spectrum), while additional pieces are used to provide Be peaks in the absorber spectra (the β spectra). It is essential to the arguments which have been presented for the data-analysis procedures associated with these two geometries that all the Be foils have the same thickness, and hence the same ionization loss. It was possible, by comparing the total areas under

TABLE III. The principal corrections for all data.

No.	Element/ geometry	Beam-width correction (keV)	Beryllium thickness correction (keV)	Absorber thickness correction (mg/cm^2)
1	C/3	2.8±0.6	0.7±0.1	0.2
2	C/3	3.8±0.6	0.7±0.1	0.1
3	C/3	4.3±0.5	0.7±0.1	···
4	C/3	6.7±1.1	0.7±0.1	···
5	C/3	4.4±0.6	0.7±0.1	0.4
6	C/2	5.6±1.1	···	···
7	C/2	4.4±1.2	8.1±1.	···
8	C/2	3.2±1.2	32.1±4.	
9	Al/3	3.6±0.8	···	···
10	Al/2	4.2±0.9	···	···
11	Al/1	6.1±1.2	···	···
12	Al/3	5.5±0.8	···	0.4
13	Al/1	9.9±1.2	···	···
14	Al/3	5.9±0.7	···	0.4
15	Al/2	4.2±0.9	···	0.5
16	Al/1	11.7±1.1	···	0.5
17	Cu/3	3.5±0.8	···	···
18	Cu/3	5.3±0.9	···	···

the Be peaks in the various spectra, to check this equality of thickness. It was discovered that one of the available Be foils was 5% thicker than the others. This foil was used to scatter electrons toward all of the thinner carbon absorbers. It will be noted in Table III that the correction for this extra 5% of Be amounted to less than 1 keV in ionization loss.

The two thickest carbon targets, which were analyzed by the geometry-2 procedure, did have beryllium foils included in the absorber spectra. It was therefore necessary to correct for the energy loss in this beryllium in order to find the energy loss in the carbon alone.

3. *Absorber thickness*

The column labeled absorber-thickness correction contains those values by which the thickness at the center of some targets was found to differ from the over-all average thickness of the target. These shifts were in all cases found to be smaller than the uncertainty in the average thickness itself.

4. *Other*

Values are not available for the exact shift in most-probable energy loss caused by radiation effects. These values were not calculated separately since the radiative unfolding routines were part of the initial data-reduction program and very few precise measurements were taken on peak positions in nonradiation-corrected spectra. The shifts introduced by the radiation correction are known to be ~5 keV, however, for targets in this thickness range at 50-MeV incident energies.

The various systematic parameters which might cause additional uncertainties in a measurement of this sort are the positioning of the detector ladder, the spacing of the detectors on the ladder, and the stability of the spectrometer and of the beam energy-defining magnets. These parameters are known from previous experiments to yield a total systematic uncertainty of ±2 keV.

C. Conclusions

Figure 10 is a plot of the percent difference between theory and experiment *vs* target thickness. The Theissen and Gudden[10] points for carbon are included. The data are in excellent agreement with the theory of Sternheimer down to ~0.1 g/cm^2. Below this point an apparent systematic deviation of the carbon data from the theoretical curve is observed. It is noticed, however, that the aluminum and copper data show no such drift away from the theoretical curve. A χ^2 analysis of the fit of all the data to the theoretical curve yields a total χ^2 of 19.2 for 17 degrees of freedom, giving a confidence level of 0.35. The carbon points alone yield a χ^2 of 12.1 for 7 degrees of freedom, giving a confidence level of 0.10.

It was not possible to make any significant statement about the comparison of measured peak shapes with theoretical predictions for the width

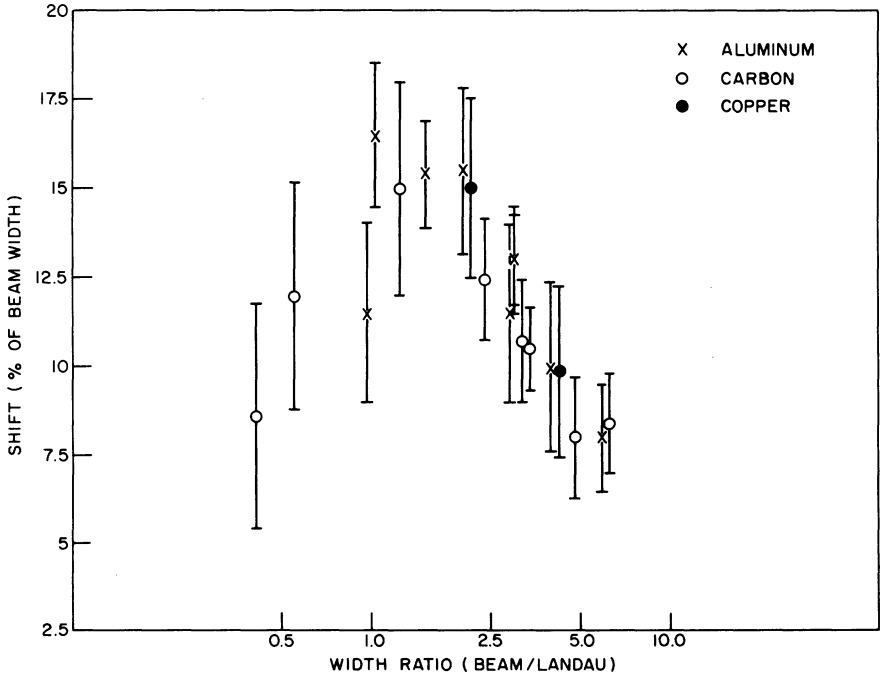

FIG. 9. The measured beam-width corrections for the experimental data.

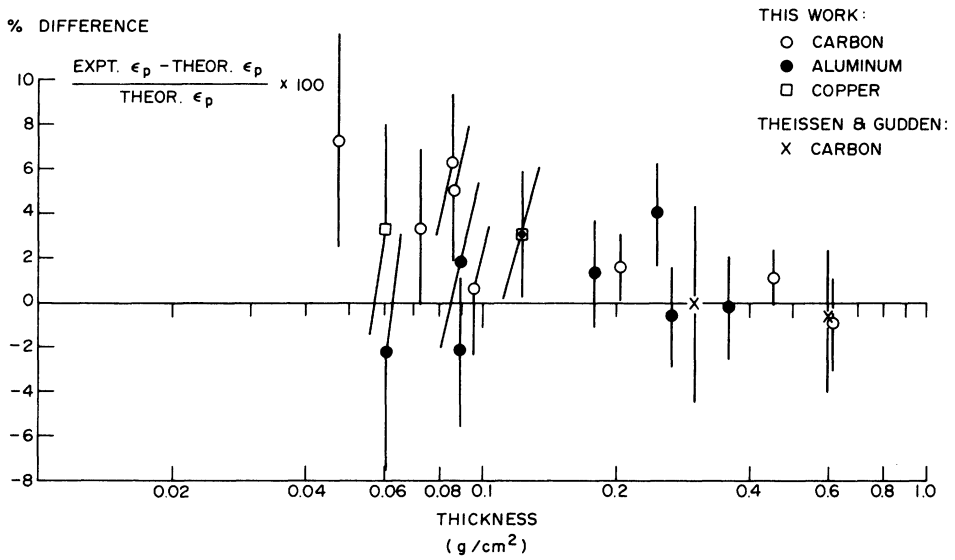

FIG. 10. A comparison of the experimental measurements of most-probable ionization loss with the theoretical predictions according to the Sternheimer formulation.

of the Landau distribution. The beam width is a much too dominant component of the observed width, for this range of thickness, to be able to make any meaningful comparison with theory.

The potential usefulness of ionization-loss measurements to provide in-beam determinations of the effective thickness of scattering targets has been demonstrated by the geometry-1 and geometry-2 results. The accuracy of such measurements depends upon several factors, principally on the actual thickness being measured and on the precision to which the momentum distribution in the incident beam is known. It is possible, as is shown in Table III, to make thickness measurements to better than ±3% on targets of thickness >100 mg/cm^2. Thicknesses of thinner targets can be measured somewhat less accurately. This technique may prove valuable; both as a check of more conventional methods of determining the thickness, and also as a satisfactory method in cases where it is not possible to obtain accurate thickness determinations by other methods.

ACKNOWLEDGMENTS

The authors wish to thank Dr. S. P. Fivozinsky, Dr. P. L. Hallowell, and Dr. J. W. Lightbody, Jr., for their assistance in collecting the data. The cooperation of the accelerator crew at the National Bureau of Standards accelerator is sincerely appreciated. We would also like to thank Dr. D. Polanski and, in particular, Don Case for their very generous assistance with the x-ray work, Dr. R. Roosen for his help with the microdensitometry, and Dr. N. L. Bonavito for his contributions to the data-analysis effort.

---

*Work supported in part by National Science Foundation grants Nos. GP-29226 and GP-34391.

†Present address: Montgomery College, Rockville, Maryland.

‡Present address: Department of Physics, University of Massachusetts, Amherst, Massachusetts.

[1]R. M. Sternheimer, Phys. Rev. 88, 851 (1952); 89, 1148 (1953); 91, 256 (1953); 103, 511 (1956); 145, 247 (1966); 164, 349 (1967); in *Methods of Experimental Physics*, edited by L. C. L. Yuan and C. S. Wu (Academic, New York, 1961), Vol. 5A, pp. 4–55.

[2]B. T. Price, Rep. Prog. Phys. 18, 52 (1955).

[3]A. Crispin and G. N. Fowler, Rev. Mod. Phys. 42, 290 (1970).

[4]E. C. Goldwasser, F. E. Mills, and A. O. Hanson, Phys. Rev. 88, 1137 (1952).

[5]B. Hildebrand, Phys. Rev. 90, 378A (1953).

[6]W. Paul and H. Reich, Z. Phys. 127, 429 (1950).

[7]E. L. Goldwasser, F. E. Mills, and T. R. Robillard, Phys. Rev. 90, 378A (1953).

[8]A. M. Hudson, Phys. Rev. 105, 1 (1957).

[9]F. A. Bumiller *et al.*, Z. Phys. 223, 415 (1969); 234, 185 (1970); J. C. Goodwin, Jr., M. S. thesis, U. S. Naval Postgraduate School, 1968 (unpublished); W. R. DeLuill and J. B. Raynis, M. S. thesis, U. S. Naval Postgraduate School, 1969 (unpublished).

[10]H. Theissen and F. Gudden, Z. Phys. 191, 395 (1966).

[11]L. Landau, J. Phys. (USSR) 8, 201 (1944); K. R. Symon,

Ph. D. thesis, Harvard University, 1948 (unpublished); B. Rossi, *High Energy Particles* (Prentice Hall, New York, 1952), pp. 22–35.
[12]H. D. Maccabee and D. G. Papworth, Phys. Lett. 30A, 241 (1969).
[13]R. M. Sternheimer and R. F. Peierls, Phys. Rev. B 3, 3681 (1971).
[14]R. D. Evans, *The Atomic Nucleus* (McGraw-Hill, New York, 1955).
[15]S. Penner, National Bureau of Standards Linac Internal Report No. 298, 1969 (unpublished); National Bureau of Standards Technical Note No. 523 (U. S. G. P. O., Washington, D. C., 1970).
[16]F. J. Kline, Ph. D. thesis, Catholic University of America, 1971 (unpublished); J. T. O'Brien, Ph. D. thesis, Catholic University of America, 1972 (unpublished).
[17]J. Schwinger, Phys. Rev. 75, 898 (1949).
[18]H. Crannell, Nucl. Instrum. Methods 71, 208 (1969).